Geotechnical Engineering
Volume 171 Issue GE2

A statistical analysis on concrete cut-off wall behaviour
Wen, Chai, Xu, Qin and Li

ice | proceedings

Proceedings of the Institution of Civil Engineers
Geotechnical Engineering 171 April 2018 Issue GE2
Pages 160–173 https://doi.org/10.1680/jgeen.17.00142
Paper 1700142
Received 04/08/2017 Accepted 23/11/2017
Published online 10/01/2018
Keywords: dams, barrages & reservoirs/statistical analysis

ice
Institution of Civil Engineers
publishing

A statistical analysis on concrete cut-off wall behaviour

Lifeng Wen PhD
Lecturer, State Key Laboratory Base of Eco-hydraulic Engineering in Arid Area, Xi'an University of Technology, Xi'an, P. R. China

Junrui Chai PhD
Professor, State Key Laboratory Base of Eco-hydraulic Engineering in Arid Area, Xi'an University of Technology, Xi'an, P. R. China; School of Civil Engineering, Xijing University, Xi'an, PR China (corresponding author: jrchai@xaut.edu.cn)

Zengguang Xu PhD
Assistant Professor, State Key Laboratory Base of Eco-hydraulic Engineering in Arid Area, Xi'an University of Technology, Xi'an, P. R. China

Yuan Qin PhD
Assistant Professor, State Key Laboratory Base of Eco-hydraulic Engineering in Arid Area, Xi'an University of Technology, Xi'an, P. R. China

Yanlong Li PhD
Professor, State Key Laboratory Base of Eco-hydraulic Engineering in Arid Area, Xi'an University of Technology, Xi'an, P. R. China

Concrete cut-off walls are a well-established technique for forming seepage cut-off in pervious and compressible foundations in newly constructed dams. This study investigated the behaviour of cut-off walls on the basis of statistical analysis. A set of monitoring records and construction details of 43 case histories of in-service concrete cut-off wall constructed in the past 50 years were gathered. Detailed statistical analyses of horizontal displacement, crest settlement, cracking behaviour and stress of the walls were performed based on the case histories. Loading characteristics and relative settlement between the wall and the alluvium foundation were analysed. The statistical analyses also attempted to identify quantitatively the major factors affecting the wall behaviour; these factors include wall location, wall material, foundation deformation characteristics, wall depth and valley shape. The wall location was found to be the deterministic factor that affects the wall behaviour. The findings and results of this study provide a significant insight into concrete cut-off wall behaviour and provide a valuable reference for future wall design and construction.

1. Introduction

Given the increase in energy demands and evolution in construction methods, an increasing number of earthen dams have been and are being founded on pervious and highly compressible alluvial deposits. Concrete cut-off walls are increasing in popularity. They are effective in controlling foundation seepage because they provide a continuous seepage cut-off and are less prone to deteriorate than other methods (Bruce *et al.*, 2012; Durgunoglu *et al.*, 2012; Kalkani and Michali, 1984; King and Collins, 1968; Moharrami *et al.*, 2014; Rosen *et al.*, 2011). During dam construction and reservoir filling, the foundation and wall compress under the weight of the dam body and water load. Consequently, the wall may undergo significant plastic straining, which potentially leads to cracking. Case studies on long-term wall performances have encountered direct evidence of cracking of the cut-off wall (Rice and Duncan, 2010a, 2010b). Rice and Duncan (2010b) reported that even cracks with apertures of less than one millimetre can increase the effective hydraulic conductivity of a seepage barrier by several orders of magnitude. Hinchberger *et al.* (2010) found that the hydraulic conductivity of plastic concrete (PC) could increase between two to three orders of magnitude due to crack formation based on traxial compression tests. Understanding wall behaviour is thus critical to design optimisation and performance assessments.

The loading characteristics of the cut-off wall are complicated. The wall not only bears the dam's gravity and the water pressure caused by the reservoir filling, but also has a complex interaction with the adjacent soil. A series of laboratory tests was performed to characterise the mechanical and hydraulic performances of cut-off wall materials (Abbaslou *et al.*, 2016; Ata *et al.*, 2015; Bagheri *et al.*, 2008; Hinchberger *et al.*, 2010), but wall behaviour was rarely tested directly (Xiao *et al.*, 2016). The technical characteristics and structural performance of the wall of several projects were presented (Brunner *et al.*, 2006; Dascal, 1979); however, a vast difference exists among various projects. Hence, only limited insights into wall behaviour could be obtained. Several investigators have performed numerical analyses on the behaviour of cut-off walls (Li *et al.*, 2015; Wen *et al.*, 2015, 2017; Yu *et al.*, 2015), but the numerical results were not validated by the measured results and in-depth analysis was not involved. Hou *et al.* (2004) performed centrifuge model tests to study cut-off wall behaviour under the complex loads condition; however, these tests cannot simulate field stress conditions. Based on the observations and insights obtained from 30 case histories of earthen dams, Rice and Duncan (2010a) investigated the failure or cracking mechanisms of the seepage barriers and gained significant insights regarding the long-term performance of such barriers. However, they focused only on seepage barriers employed to repair existing dams. Many cut-off walls have been built in dam alluvium foundation, but studies on the wall behaviour remain limited. Extensive studies are necessary to understand the behaviour of concrete cut-off walls.

In this paper, a considerable effort has been made to collect the behaviour recorded in case histories of concrete cut-off walls and thus conduct sound statistical analysis. Data on monitoring records, construction details and foundation characteristics were gathered for 43 in-service concrete cut-off walls. The main objective of this study is to analyse the concrete cut-off wall behaviour from the statistical point of view. Some aspects of the current state of practice for concrete cut-off wall construction are first discussed. Then detailed statistical analyses of horizontal displacement, crest settlement, cracking and stress of the walls are conducted. Close attention is also given to the effect of various factors including wall location, wall material, foundation deformation characteristics, wall depth and valley shape on the behaviour of the cut-off wall.

2. Current practice in the concrete cut-off wall and case history database

2.1 Current practice

A concrete cut-off wall has numerous advantages over other techniques, such as excellent impermeability, adaptability to geology and real-time monitoring of construction quality. The wall thickness generally varies in the range 0·6–1·2 m, depending mainly on dam height. A cut-off wall is usually required to penetrate a minimum of 0·5–1·0 m into the bedrock or a relatively impermeable layer. In some projects, suspended walls are constructed because of the deep thickness (more than 70 m) of the alluvium. An increasing number of the walls are being built using PC, which comprises cement aggregate and water mixed with bentonite. Compared with ordinary concrete (OC), the bentonite added in PC makes this material more deformable. The construction method of a PC wall is similar to that of an OC wall, but the material characteristics of the PC make the construction method of the PC wall more complicated. In general, a PC mix experiment should be conducted in accordance with the design requirements before the construction of the wall. Compared with an OC wall, the PC wall has different test methods for material performance parameters and wall quality inspection methods. The conventional construction method of the OC wall is outlined below.

The slot-type wall is the main form for the cut-off wall (Moharrami *et al*., 2014; Song and Cui, 2015). The construction technique for OC walls varies widely depending on the wall depth, nature of foundation materials and available technologies. OC walls are commonly constructed in discrete elements, such as panels or large-diameter piles (Arnold *et al*., 2011; Brunner *et al*., 2006; Durgunoglu *et al*., 2012; Gularte *et al*., 2007). The stop-end pipe is the most commonly used method for providing a construction joint between every two successive panels (Brown and Bruggemann, 2002; Song and Cui, 2015). Figure 1 displays a typical OC wall construction procedure adopting panel-by-panel technique and stop-end pipe method. The construction process can be divided into two phases. First, several primary panels are constructed with a space between them. Then, secondary panels are constructed and inserted in the space when the primary panels reach the required strength. Panel alignment, deviation, trench stability, joint cleanliness and concrete segregation must be considered in construction to prevent defects.

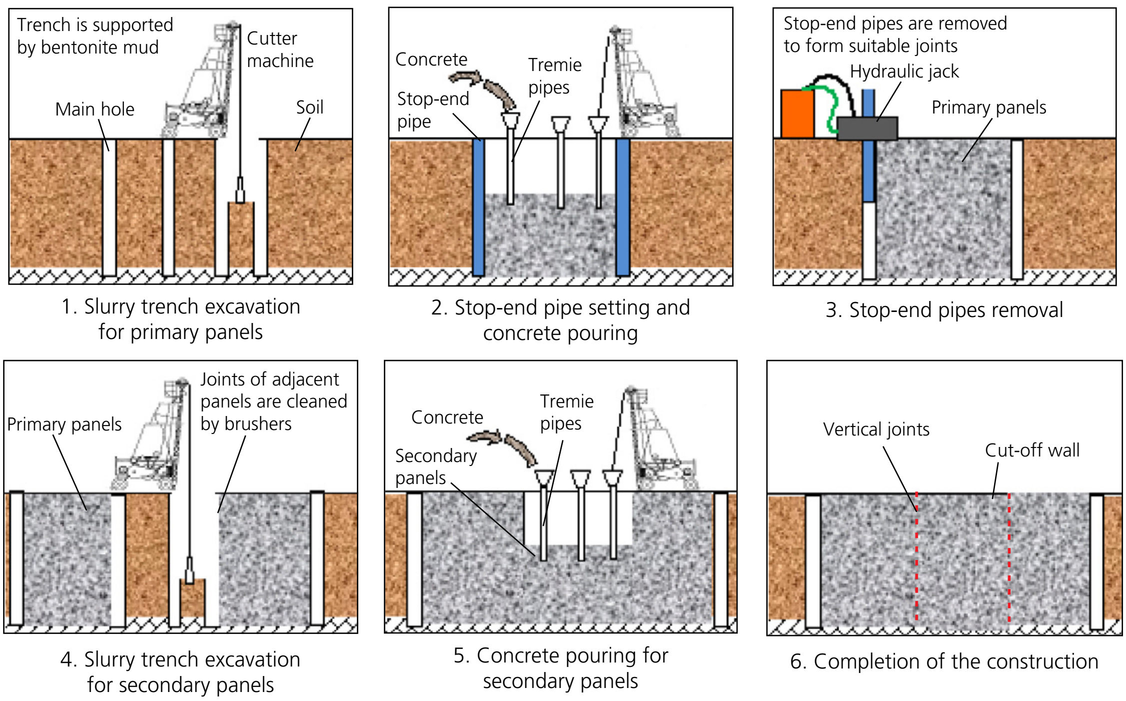

Figure 1. Typical OC cut-off wall construction procedure adopting panel-by-panel technique and stop-end pipe method

Selecting the proper time to extract the stop-end pipe and define the withdrawal force of the stop-end pipe is an important concern when using the stop-end pipe method. Song and Cui (2015) reported the waiting time prior to the removal of the stop-end pipes should occur after the initial setting time of the concrete. The stop-end pipe self-weight, interaction force between the pipe and concrete, friction between the pipe and side walls, and stop-end pipe inclination have the most significant effects on the withdrawal force. Observations and experience from the construction of walls have shown that a small thickness of bentonite infill from the bentonite slurry used during excavation usually adheres to the side walls of the primary panels (Brown and Bruggemann, 2002; Soroush and Soroush, 2005). Soroush and Soroush (2005) concluded that the primary panel age, slurry cement content, quantity of additives in the slurry and circulation as opposed to non-circulation of the slurry are responsible for the bentonite infill thickness based on a series of physical model tests.

2.2 Case history database

To conduct a sound statistical analysis, in this study a lot of effort has been directed to collecting cut-off wall behaviour cases. A database on the concrete cut-off wall behaviour of 43 cases in the past 50 years was collected from published papers, unpublished reports and monitoring data. The cases are from 14 countries, with China represented in 24 cases. Information on the characteristics of the dams and the characteristics and deformation behaviour of the foundation and cut-off wall were collected. Table 1 present the details of the 43 cases for wall behaviour analysis. Dam types included in this study are concrete face rockfill dam, dams with inclined wall, dams with core walls, homogeneous dams and dams with inclined core walls, where concrete face rockfill dams and dams with core walls comprised most of the cases, both at 37·2%. In this research, the location of the cut-off wall was divided into two categories, namely, at the upstream toe of the dam (UD) for concrete face rockfill dam and dams with inclined wall, and at the middle bottom of the dam (MD) for dams with core walls, homogeneous dams and dams with inclined core walls. The height variation of most dams is 50–125 m, with an overall range of 35·4–186 m. The foundation valley can be U-shaped or V-shaped.

The alluvium foundation in the database is mainly composed of sand and gravel, gravel and fine sand. The thickness of most alluvium ranges from 30 to 80 m. The dry density (ρ_d), foundation bearing capacity (f) and foundation deformation modulus (E_0) of the alluvium are generally in the range of 2·0–2·2 g/cm^3, 0·40–0·60 MPa and 40–65 MPa, respectively. The foundation bearing capacity (f) refers to the allowable load on a unit area of the foundation under the conditions to meet the stability of the foundation and the requirement that the foundation deformation does not exceed the allowable value. According to the suggestion provided in the hydraulic power specification SL237 (WaterPower, 1998) in China, the foundation bearing capacity is determined by the empirical relationship ($f = 35{\cdot}96\text{N}63{\cdot}5 + 23{\cdot}8$) between f and the heavy dynamic penetration index (N63·5). N63·5 is the required number of hammer blows for the probe to penetrate 10 cm into the foundation using the dynamic penetration test. The dynamic penetration test uses a steel hammer with weight of 63·5 kg, and this steel hammer free falls from the height of 76 cm in each hammer blow movement. The foundation deformation modulus (E_0) is the ratio of vertical stress increment to the corresponding strain increment under unconfined conditions and is an important index for foundation compression deformation. This modulus reflects the capability of soil to resist elastoplastic deformation. The E_0 is generally determined by in situ tests, including a pressure-meter test, dynamic penetration test and a plate-loading test. In the pressure-meter test, E_0 is determined by a pressure–volume relationship curve on an empirical basis (CSHE, 2007). The empirical relationship between E_0 and the dynamic penetration index is used to determine E_0 in the dynamic penetration test (Li *et al.*, 2007). In the plate-loading test, E_0 is determined by a pressure–settlement relationship curve (CSHE, 2007).

The wall depths vary over a range of 13·4–131 m. Most of the walls penetrated into the bedrock or relatively impermeable layer; however, suspended walls were constructed in some cases (numbering ten cases). The collected walls were mostly constructed using OC, with only nine cases constructed using PC. The settlements of the foundation surface after reservoir filling adjacent to the downstream face of the wall of some cases were collected. The settlement of the wall crest and the foundation surface were mainly measured using hydraulic overflow settlement gauges (measurement range: 1·0–3·5 m, system accuracy: ≤0·4%FS (full scale)). Fixed inclinometers (measurement range: ±30°, system accuracy: ≤0·1%FS) were always installed in the cut-off walls for measuring horizontal displacements. The wall horizontal displacement both at the end of dam construction (EOC) stage and after the end of the reservoir filling (EOF) stage were collected. The horizontal displacements of the walls were calculated by the measured tilt angle of the walls.

The behaviour of a positive cut-off is generally evaluated through its efficiency as far as seepage is concerned. The efficiency of the cut-off wall as a seepage barrier based on case history data has been rarely reported because of the difficulty in assessing leakage in deep, permeable deposits below an earthen dam (Brown and Bruggemann, 2002). In order to evaluate the efficiency of the cut-off wall, leakage rate records of some cases have been collected in Table 1. The leakage rate refers to the amount of water exuded from the downstream of the dam and is measured using a weir installed on the downstream of the dam. As showed in Table 1, most of the collected case histories exhibit leakage rate of 60 l/s or smaller; however, the Jiudianxia dam (136 l/s) and Arminous dam (130 l/s) exhibit a large leakage rate. Such a large leakage rate may be due to the large dam height and foundation thickness of the Jiudianxia dam and vertical joints cracks and erosion of the

Table 1. Select details and deformation measurements for foundation and concrete cut-off wall of 43 in-service dams

No.	Project	Country	Year	H: m	Dam type and L: l/s	VS	Foundation properties						Cut-off wall properties								Ref.
							GC	FT: m	ρ_d: g/cm^3	f: MPa	E_0: MPa	FS: cm	D: m	T: m	A: 10^{3}m^2	Material and E_c	D_1: cm	D_2: cm	CS: cm	FS/CS	
1	Lianghui	China	2002	35·4	CFRD, 60	U	SG	31	2·18	0·45–0·50	60–65	6·9	31·7	0·8	65·8	OC	–4·9	10·2	1·6	4·3	R4
2	Meixi	China	1998	41	CFRD	U	SP	30	2·00	—	—	—	30·5	0·8	10·5	OC, 17 GPa	–5·0	5·4	—	—	R9
3	Kekeya	China	1981	42	CFRD, 20	U	SG	37·5	—	—	60	4·9	37·5	0·8	5·4	OC	—	—	1·2	4·1	R4
4	Yunzhou	China	1994	43	DI, 31	V	SG	50	2·12–2·20	0·45–0·50	55–60	—	50	0·8	5·4	OC	–6·6	7·1	—	—	R4
5	Qiaodun	China	1984	50	DI	V	SG	43	2·00–2·10	0·55–0·60	50–55	5·1	45	0·8	8·1	OC	–6·2	8·9	1·6	3·2	R7
6	Dahe	China	1998	50·8	CFRD	—	G	37	2·05	0·35–0·45	55–60	3·0	38	0·8	—	OC, 28 GPa	–1·4	3·5	0·9	3·3	R9
7	Renzonghai	China	2008	56	DI, 43	U	G	148	2·10	0·30–0·60	25–50	5·4	82	1·0	—	OC, 28 GPa	–9·1	5·2	1·7	3·2	R16
8	Hanpingzui	China	2004	57	CFRD, 95	U	SG	40	2·15	—	—	—	41	0·8	2·8	OC, 15 GPa	–3·1	7·3	—	—	R14
9	Ravi	Mexico	1968	60	DI	U	SG	80	—	—	50–55	77·4	13·4	0·6	15	OC	—	—	2·8	4·8	R14
10	Longtoushi	China	2007	72·5	DI, 44	—	SG	70	2·20	0·50–0·60	55–60	12·8	70	0·8	—	OC	–8·6	7·3	2·1	6·1	R14
11	Puclaro	Chile	1999	83	CFRD	—	SG	113	2·00–2·15	0·40–0·60	50–60	6·5	60	0·8	12·1	OC	–9·5	4·2	1·3	4·9	R8
12	Laodukou	China	2009	96·6	CFRD	V	SG	29·6	2·00	0·45–0·50	45–55	2·4	30	0·8	10·7	OC, 26 GPa	–4·0	4·5	0·6	4·0	—
13	Xieka	China	2014	108·2	CFRD	V	G	100	2·10–2·20	0·50–0·60	45–50	—	70	1·2	5·6	OC	–5·9	2·8	—	—	—
14	Nalan	China	2005	109	CFRD, 95	U	G	24·3	2·19	0·50–0·60	33–45	5·2	24·8	0·8	—	OC, 18 GPa	–2·9	6·5	0·8	6·5	R10
15	Chahanwushu	China	2009	110	CFRD, 15	U	SG	46·7	2·14	0·50–0·60	45–55	8·9	47·7	1·2	10·2	OC, 28 GPa	–13·5	12·9	2·1	4·2	R15
16	Miaojiaba	China	2011	110	CFRD	V	SG	48	2·15–2·20	0·55–0·60	60–65	8·2	48·5	1·2	2·9	OC, 26 GPa	–6·8	9·9	2·0	4·1	R15
17	Jinchuan	China	2012	112	CFRD	—	SG	65	2·24	0·55–0·60	40–45	6·8	66	1·2		OC	—	—	1·8	3·8	—
18	Duonuo	China	2012	112·5	CFRD	V	CG	35	2·17	0·50–0·55	50–60	8·6	30·5	0·8	—	OC, 26 GPa	–2·0	6·3	2·4	3·6	—
19	Santa Juana	Chile	1995	113·4	CFRD, 50	U	SG	30	2·10	—	—	1·3	30	0·6	8·9	PC	—	—	1·3	0·9	R6
20	Zoccolo	Italy	1965	116·5	CFRD	V	G	100	2·00–2·20	—	—	—	55	0·8	33·1	OC	–7·4	6·5	—	—	R14
21	Jiudianxia	China	2008	136	CFRD, 136	V	SG	56	1·95–2·12	0·50–0·60	40–60	10·0	57·8	1·2	8·9	OC, 28 GPa	–11·3	20·3	2·1	4·8	R17
22	Brombach	Germany	1985	40	HD	U	G	40	1·95–2·15	0·40–0·50	40–50	—	40	0·6	12·5	PC	2·3	5·6	—	—	R8
23	Atbara	Sudan	2013	40	DC	U	CG	20	2·20	0·55–0·65	40–45	51·4	21	0·6	11·2	OC, 28 GPa	—	5·9	7·8	6·6	—
24	Aromos	Chile	1979	42	DC, 35	U	CG	22	2·00	0·45–0·50	45–55	16·2	22·5	0·8	—	PC	1·1	5·7	15·0	1·1	R11
25	Verney	France	1982	42	HD	U	G	75	2·10–2·15	0·45–0·50	45–55	12·6	50	1·2	13	PC	–0·6	9·7	12·1	1·0	R11
26	Arminous	Cyprus	1999	42	DC, 130	V	SG	15	—	—	—	2·0	16	0·8	0·4	PC	—	—	1·9	1·9	R2
27	Penitas	Mexico	1984	45	DC	—	SG	55	2·16	0·45–0·50	55–60	9·5	55	0·8	—	PC	—	—	5·6	1·7	R3
28	Poeijos	Peru	1973	48	DC, 57	U	G	48	2·15	—	45–50	—	47	1·0	5·6	OC	–2·1	6·2	—	—	R3
29	Allegheny	America	1964	51	DC	U	—	55	2·15	—	55–60	56·7	56	0·7	10·7	OC	—	—	9·3	6·1	R7
30	Gattavita	Colombia	1963	54	DIC	—	—	92	—	—	—	—	78·6	0·8	—	OC	–2·3	4·6	—	—	R7
31	Boulder	England	1968	55	DC	V	—	46	—	—	50–55	60·4	46·4	0·6	8·2	OC	0·8	7·6	8·5	7·1	R6
32	Wanan	China	1985	64·5	DC, 42	U	SG	44	2·15	0·50–0·55	50–55	75·0	44·5	0·8	14·9	OC	–1·3	7·9	15·0	5·0	R14
33	Evretou	Cyprus	1988	70	HD	V	SG	40	—	—	—	34·0	40	0·8	2·1	PC	–2·2	4·6	17·0	2·0	R11
34	Xiabandi	China	2009	81	DC, 47	U	G	148	1·95	0·45–0·60	45–55	40·1	80	1·0	20·1	PC	1·0	4·6	37·0	1·3	R17
35	Jinping	China	2010	91·5	DC, 51	V	SG	85	1·80–2·06	—	—	—	80	1·2	—	OC, 23 GPa	–2·8	10·0	—	—	—
36	Big Hotn	Canada	1972	92	DC	V	SG	65	—	0·45–0·55	55–60	88·2	65	0·6	3·2	OC	–1·0	8·9	12·6	7·0	R13
37	Bikou	China	1998	101	DC, 49	U	SG	34	2·14	—	—	—	35	0·8	7·8	OC, 18 GPa	–2·6	4·5	—	—	R14
38	Manic 3	Canada	1976	107	DC	V	SG	126	2·04	0·50–0·60	50–60	150·0	131	0·6	20·7	OC, 28 GPa	–5·0	28·5	14·0	10·7	R5
39	Taleghan	Iran	2006	110	DC	—	SG	60	2·25	—	45–55	63·6	63	1·5	–	OC, 30 GPa	–0·2	5·2	12·0	5·3	R1
40	Colbum	Chile	1984	116	DC	U	G	68	—	—	—	10·4	68	1·2	12·8	PC	–1·6	5·4	8·7	1·2	R12
41	Yele	China	2005	125	DC, 33	—	G	420	1·94–2·24	0·55–0·60	45–60	95·7	84	1·0	55·0	OC, 25 GPa	1·1	7·8	15·2	6·3	R4
42	Xiaolangdi	China	2001	154	DIC	U	SG	73	2·10–2·15	0·55–0·60	60–65	40·0	70·3	1·2	21·2	OC, 30 GPa	–5·1	20·0	8·1	4·9	R14
43	Pubugou	China	2010	186	DC	V	G	75	2·14–2·20	0·50–0·65	60–65	40·0	76·8	1·2	6·2	OC, 26 GPa	–3·5	7·0	11·0	3·6	—

H, dam height; L, leakage rate after reservoir filling; CFRD, concrete face rockfill dam; DI, dams with inclined walls; DC, dams with core walls; HD, homogeneous dams; DIC, dams with inclined core walls; VS, foundation valley shaped; GC, ground condition; SG, sand and gravel; SP, sand and pebble; G, gravel; CG, crushed gravel; FT, thickness of the alluvium foundation; ρ_d, dry density; f, foundation bearing capacity; E_0, foundation deformation modulus; FS, settlement of the foundation surface adjacent to the downstream face of the wall after the EOF stage; D, depth of the wall; T, thickness of the wall; A, area of the wall; E_c, elastic modulus of the concrete; PC, plastic concrete; OC, ordinary concrete; D_1, maximum horizontal displacement at the top of the wall at the EOC stage, downstream direction (+); D_2, maximum horizontal displacement at the top of the wall after the EOF stage; CS, maximum crest settlement of the wall after the EOF stage; the heading of year means the year of end of dam construction. R1, Arnold *et al*. (2011); R2, Brown and Bruggemann (2002); R3, Brunner *et al*. (2006); R4, CSHE (2007); R5, Dascal (1979); R6, Fell *et al*. (2005); R7, Gao (2000); R8, Hunter (2003); R9, Hou *et al*. (2004); R10, Li *et al*. (2007); R11, Rice (2007); R12, Rosen *et al*. (2011); R13, Soroush and Soroush (2005); R14, Wang *et al*. (2008); R15, Wen *et al*. (2015); R16, Yu *et al*. (2015); R17, Gan *et al*. (2014)

Arminous dam. Won and Kim (2008) reviewed the long-term leakage rate of 27 earthen dams built on rock foundations and found that the leakage rate was less than 50 l/s when the dam height was less than 125 m. A leakage of a few tens of litres per second for an earthen dam has negligible economic value (Won and Kim, 2008). The collected leakage rate in Table 1 is slightly larger than that of dams built on rock foundation and fall within the general and acceptable range, especially when the dam height is less than 125 m. This finding indicates that the cut-off wall can effectively control seepage in the foundation.

2.3 Loads acting on the cut-off wall

The behaviour of the cut-off wall is mainly determined by the horizontal and vertical loads acting on the wall. Most of the loads affecting the behaviour are indeterminate. The load characteristics of the wall located at the UD are different from that of the wall located at the MD. Figure 2 provides a schematic representation of the applied force on the wall due to the boundaries at the EOF stage.

Horizontal loads mainly include water head and lateral earth pressure. The water head pressure is related to the free surface of the seepage flow, which is mainly present after the start of reservoir filling. The lateral earth pressure is mainly caused by the horizontal displacement of the foundation, which is directly related to the placement and compaction of the dam body. The distribution of the lateral earth pressure along the wall is always non-linear with depth. Singh *et al*. (2006) proposed a detailed methodology for quantifying the resultant thrust that acts on a rigid wall. But the approach can only be used for rigid walls and a flexible levee base.

Vertical loads mainly include the self-weight of the wall, vertical earth pressure, vertical water pressure and shear force. Vertical earth pressure principally refers to the pressure generated by the filling at the top of the wall and is mainly present in the wall at the MD. Similarly, vertical water pressure is mainly present in the wall at the UD. Given that the compressibility of the walls is much smaller than that of the adjacent soil, a large settlement difference can be generated between them because of the top pressure, which causes a significant shear force at the interfaces. The observed results show that the vertical stress in the cut-off wall for a dam with core wall is larger than the upper vertical earth pressure (Brown and Bruggemann, 2002). The pressure measured in the soil adjacent to the wall is generally lower than the overburden pressure (O'Neal and Hagerty, 2011). These results indicate that the shear force is the critical load that affects the wall behaviour. Dascal (1979) concluded that 85% of the vertical stresses in the wall at the MD are induced by shear force. Shear force is mainly determined by the relative settlement and lateral earth pressure. At the upper part of the wall, the downward shear force is generated by the relative upward movement of the wall. As the depth increases, the relative displacement and shear force decrease gradually. The movement of the cut-off wall is composed of compression deformation and rigid body movement. Therefore, the settlement at the bottom of the wall may be greater than that of the alluvium. The downward shear force is reduced to zero at the depth where the wall and the alluvium are equally settled. This depth is called the neutral point. Below this depth, an upward shear force is generated. It is notable that the alluvium near the wall upstream face may move upward relative to the wall at the UD during dam construction (Wen *et al*., 2015), so an upward shear force would be generated, as shown in Figure 2.

3. Horizontal displacement of concrete cut-off walls

This section presents a review of the deformation behaviour of the concrete cut-off walls on the basis of the collected observations. Figure 3 presents the relationship between the

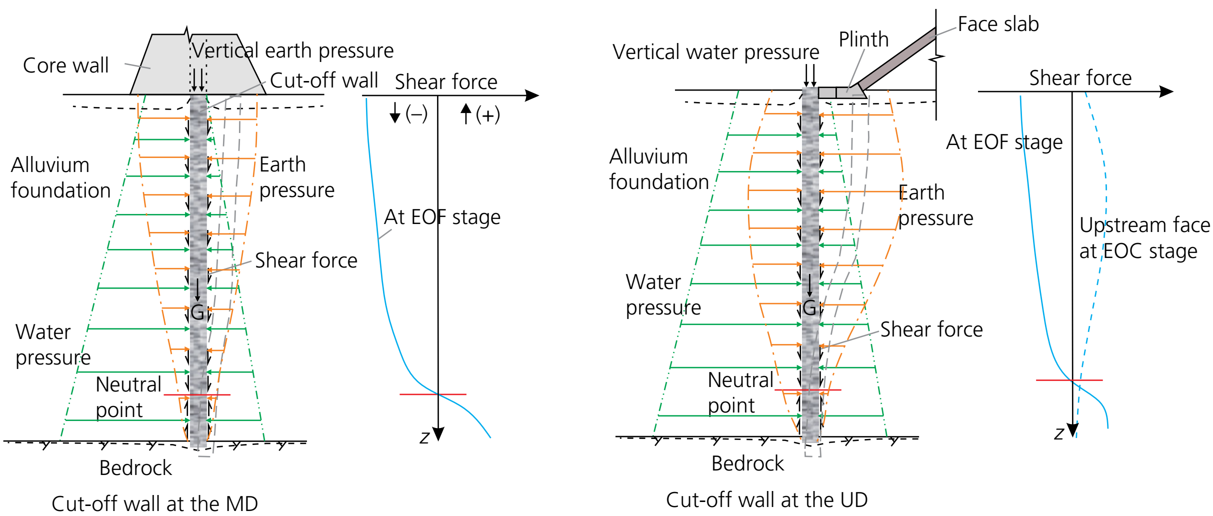

Figure 2. Schematic representation of the applied force on the wall due to the boundaries at the EOF stage

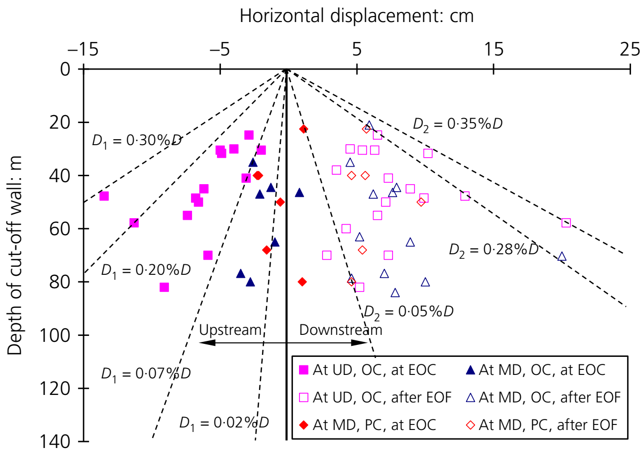

Figure 3. Relationship between the maximum horizontal displacement and the cut-off wall depth. D, depth of the wall; D_1, maximum horizontal displacement at the top of the wall at the EOC stage, downstream direction (+); D_2, maximum horizontal displacement at the top of the wall after EOF stage

maximum horizontal displacement measured in the 43 cases and the height of the wall. The wall presents generally an upstream movement during dam construction and a downstream movement after reservoir filling. However, several walls at the MD present a downstream movement at the EOC stage; these occurrences might have been caused by some walls being located on the downstream side of the centre axis. The maximum horizontal displacement for the wall at the UD is approximately 2·0–13·5 cm at the EOC stage and 3·0–13·0 cm after the EOF stage, while that for the wall at the MD is approximately 1·0–3·5 and 4·5–10·0 cm, respectively. However, several dams, such as Jiudianxia (20·3 cm), Manic 3 (28·5 cm) and Xiaolangdi (20 cm), exhibited relatively larger displacements after the EOF stage, which is likely to be due to the low-strength alluvium, ultra-deep alluvium and large dam height, respectively.

Notably, the horizontal displacement generally increases with the increase of wall depth, although the correlation is still unclear. The horizontal displacement is less than 0·30%D (where D is wall depth). Most of the horizontal displacements for the walls at UD at the EOC stage are between 0·07%D and 0·20%D (0·14%D on average), similar to 0·05%D–0·35%D (0·17%D on average) after the EOF stage. Attempts to incorporate other factors that affect the deformation result in a high degree of data variability. Except for several downstream direction displacements, the horizontal displacement for the walls at MD ranged from 0·02%D to 0·07%D (0·04%D on average) at the EOC stage in the upstream direction, which is significantly smaller than those after the EOF stage, which range from 0·05%D to 0·28%D (0·15%D on average). The horizontal displacement for the walls at UD at the EOC stage is 0·10%D larger than that for the walls at MD on average. The horizontal displacement of the wall at UD after reservoir filling is similar to that of the wall at MD. These results can be explained by examining the horizontal loads of the wall. For the wall at the MD, the horizontal displacement of the surrounding foundation soil is small, and the lateral earth pressure on the upstream and downstream surfaces of the wall is relatively small and basically symmetrical at the EOC stage. However, for the wall at the UD, a large differential lateral earth pressure can be generated from the large horizontal displacement of the surrounding foundation soil. Differential water head pressure was mainly responsible for the horizontal displacement of the wall after reservoir filling. In addition, no significant difference of the horizontal displacement was found between the walls constructed using PC and OC because the horizontal displacement is determined by the movement of adjacent soil.

Figure 4 presents the measured horizontal displacement of the cases as a function of time. The time at the start of reservoir filling for each case was set as the reference time to unify the construction stage of different dams and allow better comparability of data. As shown in the figure, the displacement increases with time before reservoir filling, but the deformation rate decreases gradually. During dam construction, approximately 70% of the total displacement occurred in the first several months, on average. The walls located at the UD exhibit relatively larger horizontal displacement compared with the walls at the MD during dam construction. The displacement gradually shifts towards the downstream direction under the effect of the water head pressure. After reservoir filling, the horizontal displacement increases over time and tends to be stable, which means that the water load has a significant effect on the wall horizontal displacement. For the time-dependent behaviour of an earthen dam, it has been reported that it takes 10–20 years for rockfill dams to be stabilised (Dounias *et al.*, 2012; Gikas and Sakellariou, 2008), which is related to rockfill and foundation characteristics, construction method and valley shape. Over 90% of the total downstream displacements occur during the reservoir filling stage, which indicates the long-term deformation of the dam and foundation has little effect on the wall behaviour. The maximum wall displacements occur at the top and near the centre because the bottom and abutments are constrained by the bedrock. Figure 5(a) presents the measured horizontal displacement distributions of several cut-off walls.

None of the collected case histories has experienced seismic shaking, so the cut-off wall behaviour under seismic loading based on case history data cannot be discussed. Evaluation of the cut-off wall behaviour under seismic loading is interesting and important work. Several researchers have conducted finite-element analysis on the seismic response of the cut-off wall (Li *et al.*, 2007; Wang *et al.*, 2008). Based on the seismic dynamic time history analysis of the cut-off wall for Jinping dam under design seismic loading, Li *et al.* (2007) reported that the

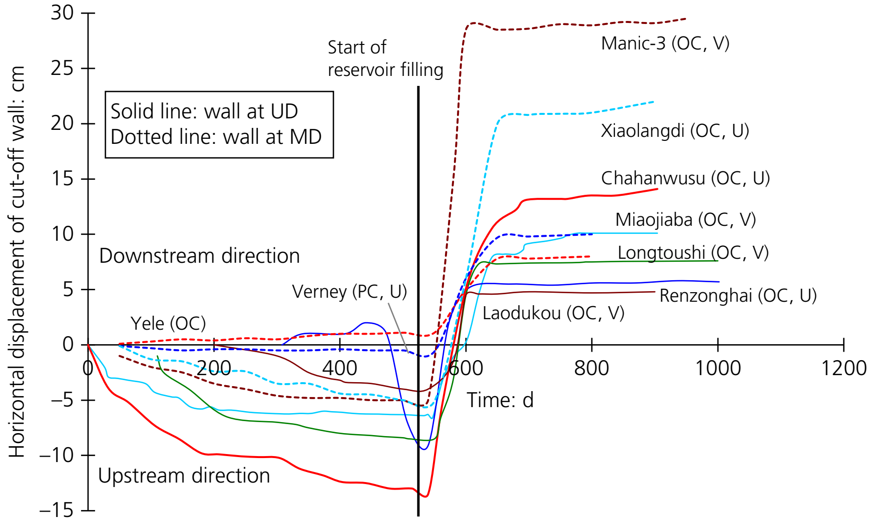

Figure 4. Evolution of the cut-off wall maximum horizontal displacement for nine cases over time. OC, ordinary concrete; PC, plastic concrete; U, V, valley shapes. A full-colour version of this figure can be found on the ICE Virtual Library (www.icevirtuallibrary.com)

acceleration in the direction along the river was relatively large. The maximum acceleration generally occurs at the top and near the centre of the wall. The dynamic displacement distribution of the cut-off wall caused by the seismic loading is basically similar to the static displacement, but the values are obviously smaller. Wang *et al.* (2008) reported that seismic loading may cause dynamic lateral tensile stress in the cut-off wall, which gradually increases from the centre of the wall to the abutments. The design seismic loading may cause the increase of the tensile stress in the wall to some extent, but the extent of the tensile and cracked region remained essentially unchanged. Seismic loading may also cause dynamic vertical compressive stress in the centre of the wall and gradually decreases from the centre to the abutments. Seismic loading induced an increase of vertical stress of the cut-off wall, but the increase was limited. In general, since the cut-off wall is located in the alluvium foundation below the dam, neither the acceleration nor the dynamic displacement responses under design seismic loading are obvious. The seismic loading does not cause significant changes in the stress state of the cut-off wall.

Figure 6 presents the normalised horizontal displacement with respect to the relative depth of the cut-off wall to the dam height. The results show that the normalised horizontal displacement for the cut-off wall at the UD and the MD both at the EOC and the EOF stage exhibit a decreasing trend with the increase of the wall relative depth. These observations can be explained as follows. As the wall relative depth increases, the deformation may increase, but the normalised deformation to the wall depth would decrease. Nearly all of the cases fall within the trend lines, except a few cases which stand out as outliers to the general trend. Suspended walls were adopted in these cases, which generate larger deformation because of the change of bedrock constraints. As shown in Figure 6, the maximum horizontal displacement for the wall at the MD varies with the wall relative depth, with a relatively smaller gradient compared with that for the wall at UD, although a regular pattern is not particularly clear. The reason for this may be that the wall at the UD mainly generates horizontal displacement.

4. Settlement of concrete cut-off walls

The settlement of the cut-off wall is a direct function of the material characteristics of the wall and the vertical loads acting upon them. Figure 7 shows the relationship between the maximum crest settlement in the cases and wall depth. As illustrated in Figure 7, for the wall constructed using OC, the maximum crest settlement after the EOF stage is generally 0·5–2·5 cm for the wall at UD and 2·0–15·0 cm for the wall at MD. Except for one scatter point, most of the settlement values for the wall at MD are between 0·10%D and 0·24%D (0·17%D on average) – significantly larger than the range between 0·02%D and 0·05%D (0·036%D on average) for the wall at the UD. The larger settlement is the result of the significant vertical earth pressure and downward shear force for the wall at the MD. However, the vertical load on the wall at the UD is smaller, because of the absence of the overlying filling. For the wall at MD constructed using PC, the settlement generally ranges from 0·18%D to 0·66%D, with an average of 0·36%D, which is twice that for the wall constructed using OC. The larger settlement is attributed to the stiffness of the PC wall, which is significantly smaller.

Figure 8 presents the measured maximum crest settlement of nine cases as a function of time, and the distribution of the settlement along the crest axis. The curves indicate that the

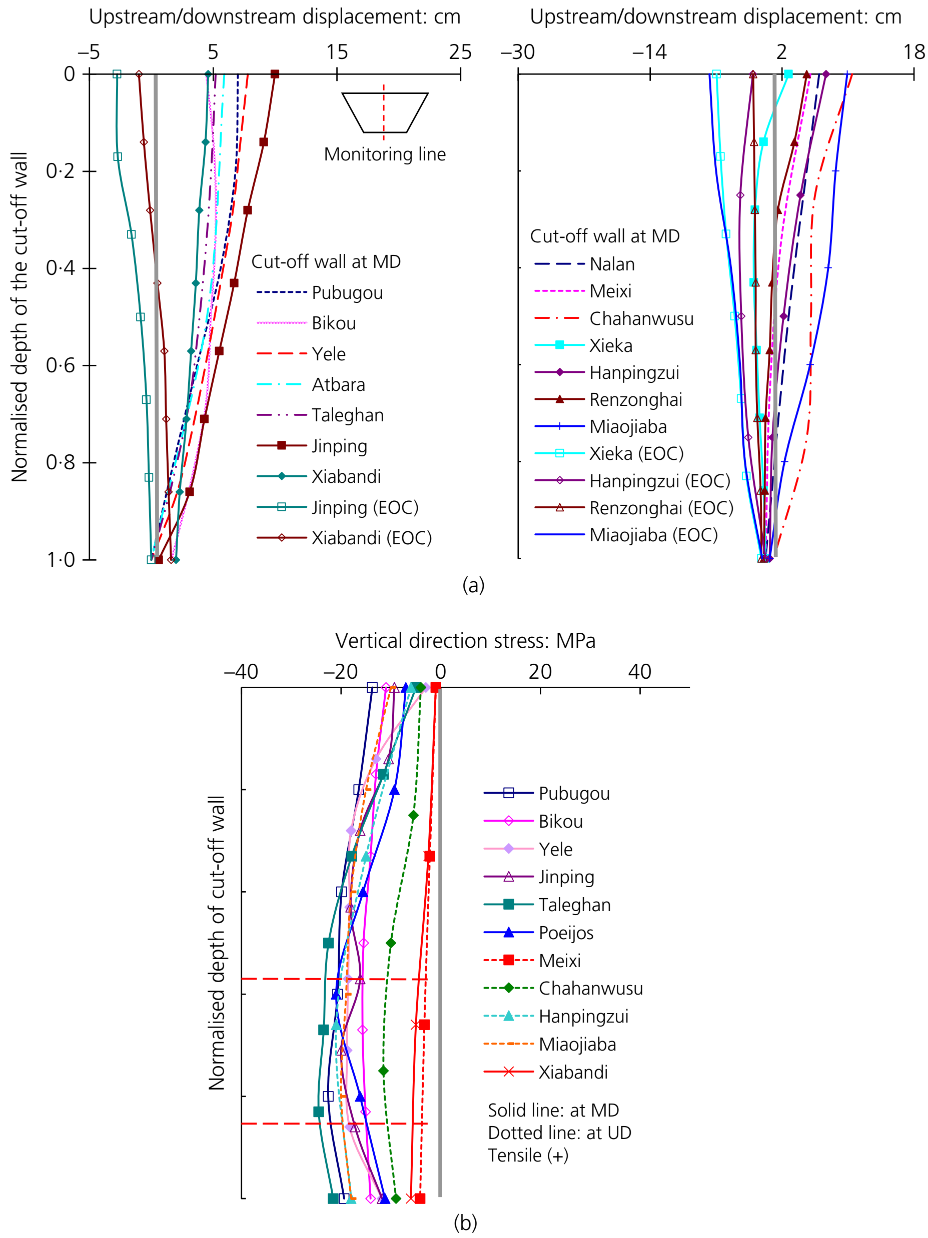

Figure 5. (a) Measured horizontal displacement and (b) compressive vertical stress distributions in downstream face of several cut-off walls at the EOF stage

settlement of the cut-off wall at the MD is considerably larger than that at the UD. Larger settlements occurred in the middle of the wall. For the wall at the MD, the settlement rapidly increased with the continuous increase in vertical loads during dam construction, but the deformation rate decreased gradually. The reservoir filling process caused increase of the settlement to some extent, but the increase rate was slower than that during dam construction. Over 80% of the total settlements occur during dam construction on average. This means that the water load has a relatively small effect on the wall settlement. As shown in Figures 4 and 8, walls constructed on a V-shaped valley exhibit relatively smaller deformation compared with walls constructed on a U-shaped valley. For example, the horizontal displacement at the EOF stage of Chahanwusu dam was 3·0 cm larger than that of Miaojiaba dam. The crest settlement at the EOF stage of Wanan dam was 2·4 cm larger than that of Big Hotn dam. This outcome is mainly caused by the more significant constraint effect of the V-shaped valley.

Figure 9 compares the maximum settlements to the maximum horizontal displacement after the EOF stage. Although no

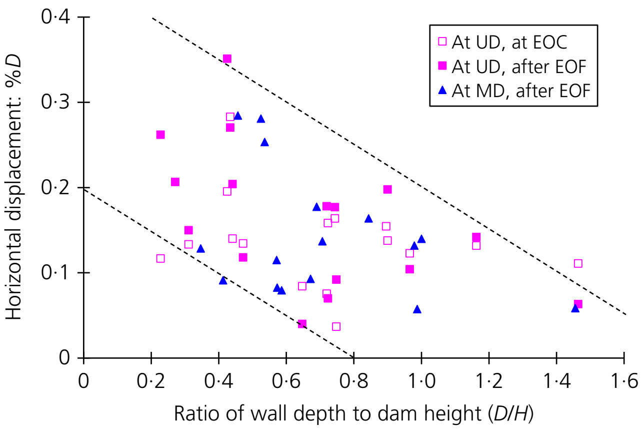

Figure 6. Measured horizontal displacement with respect to the ratio of wall depth to dam height

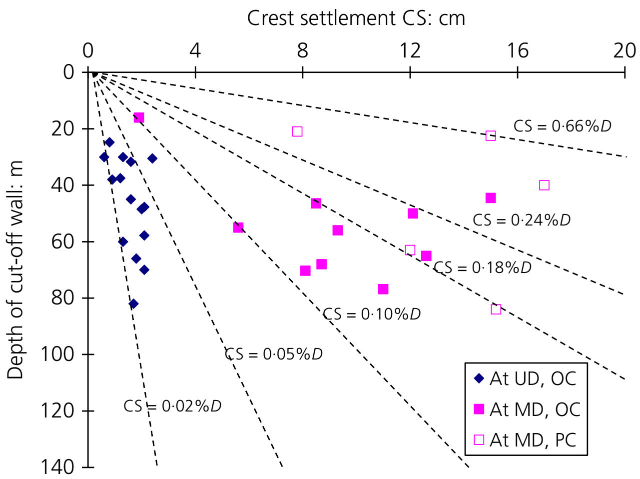

Figure 7. Relationship between the crest settlement measured in the cases and the cut-off wall depth

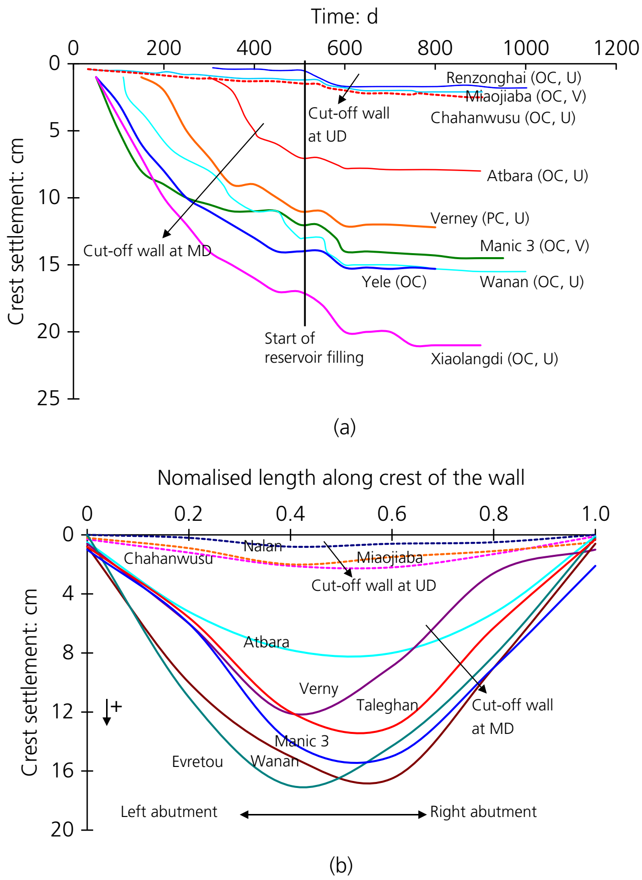

Figure 8. (a) Evolution of the wall maximum crest settlement over time; (b) measured settlement along crest axis at the EOF stage

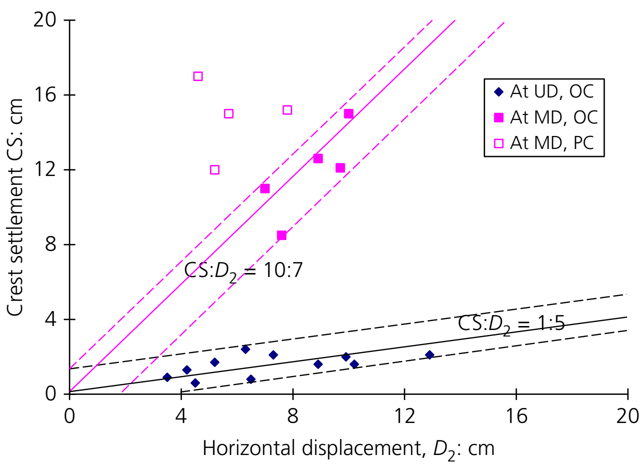

Figure 9. Comparison of the cut-off wall crest settlement and horizontal displacement after the EOF stage

direct correlation is found, some interesting observations can be obtained from the figure. The crest settlement is approximately 20% of the horizontal displacement for the wall at the UD. All data points fall within the bounds in the plot. These results indicate that the walls at UD mainly generate horizontal displacement. The crest settlement is approximately 1·4 times the horizontal displacement for the wall at MD constructed using OC and on average 2·5 times the horizontal displacement for the wall constructed using PC.

The shear force acting on the wall is closely related to the relative settlement between the wall and adjacent soil. All the alluvial foundations in the database are made of gravel or sandy gravel, leading to a relatively limited deformation compared to silty or clayey alluvium. Figure 10 presents the ratio of settlement of the foundation surface adjacent to the wall downstream side and the wall crest settlement after the EOF stage with respect to the classification of dam types and classification of foundation deformation modulus to examine the relative settlement. The relative settlement for the OC wall gradually increases with the location of the cut-off wall close to the centre, except for a few points. The observed relative settlement ratio is approximately 5–7 for the wall at MD, which is larger than the ratio of 3–5 for the wall at the UD. The ratio for the wall at MD is 1·5 times that for the wall at UD, on average. These observations can be explained by the much larger settlement in the middle of the foundation than in the upstream side. The larger relative settlement could cause a larger downward shear force, thereby causing crushing damage. Figure 10(b) shows that the relative settlement exhibits a gradually decreasing trend with the increase of E_0, which may induce a reduction of the shear force. The relative stiffness of the wall and adjacent alluvium can significantly affect the shear force by direct shear transfer. In addition, as shown in Figure 10(a), walls constructed using PC exhibit a significantly smaller relative settlements ratio, with the value of 1–2, which indicates that the deformation of the wall is generally consistent with the adjacent soil. The wall and soil together bear the vertical earth pressure because the elastic modulus of PC is low, and a small shear force will be generated. It might be expected that the shear force acting on the PC wall would significantly decrease both at the EOC and the EOF stage due to the reduction of the relative settlement compared with that of the OC wall.

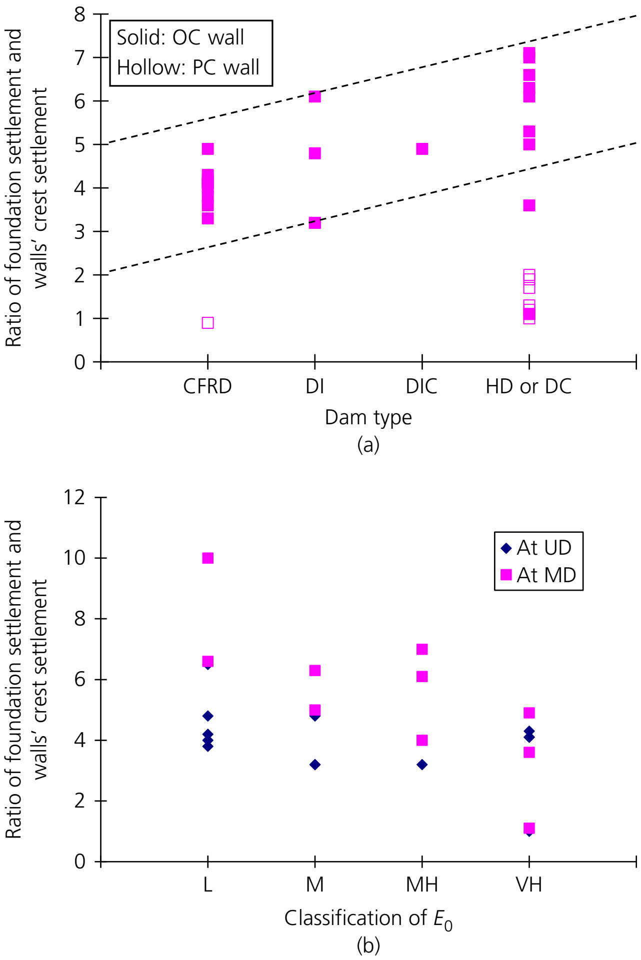

Figure 10. Ratio of settlement of foundation surface adjacent to the wall downstream side and wall crest settlement after the EOF stage with respect to (a) classification of dam type (CFRD, concrete face rockfill dam; DI, dams with inclined walls; DC, dams with core walls; HD, homogeneous dams; DIC, dams with inclined core walls) and (b) classification of foundation deformation modulus E_0 (L, $E_0 < 50$ MPa; M, $E_0 = 50–55$ MPa; MH, $E_0 = 55–60$ MPa; VH, $E_0 > 60$ MPa)

The effect of the foundation deformation characteristics on the cut-off wall crest settlement was further analysed, as shown in Figure 11. The normalised crest settlement decreases with the increase of the E_0. Nearly all of the cases are within the trend lines. The normalised crest settlement constructed on L-strength foundation is 2·9 times that on MH-strength foundation on average. These results can be explained in that the relative settlement between the wall and the foundation is small when the relative stiffness between them is small, as shown in Figure 10(b), which results in a reduction of the shear force. Li *et al.* (2007) performed a numerical calculation to study the effect of the foundation deformation characteristics on the wall behaviour. They found that the cut-off wall horizontal displacement and settlement are almost inversely proportional to E_0. Also, the greater the stiffness of the alluvium, the smaller the cut-off wall stress, especially for vertical stress. These observations indicate that the relative stiffness of the wall and alluvium has a significant effect on the wall behaviour.

5. Stress in concrete cut-off walls

Figure 5(b) presents the measured vertical stress distributions at the downstream face of some walls at the EOF stage. Large portions of the cut-off walls are in the compressive stress state. The stresses for the walls at the MD are significantly larger than those for the walls at the UD, except for Xiabandi wall,

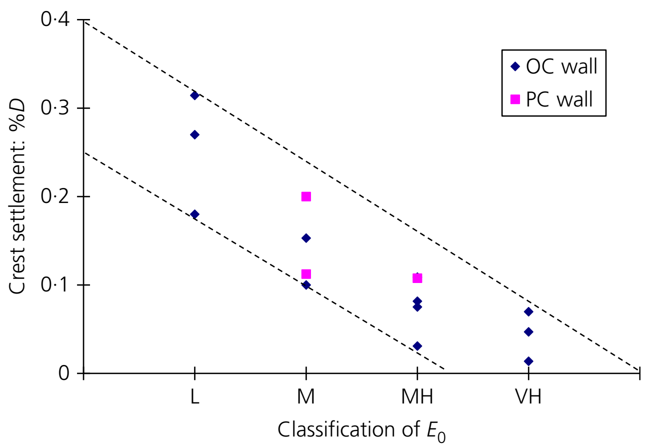

Figure 11. Measured crest settlement of the walls at the MD after the EOF stage with respect to classification of foundation deformation modulus E_0

which exhibits lower stress. The small stress may be the result of the PC material adopted. The vertical stress for the wall constructed using PC was reported as only 1/10–1/15 of that for the wall using OC (Li *et al.*, 2007). The stresses increase from the top down to a certain depth. Below this depth, the stresses start to decrease towards the bottom. The maximum compressive vertical stress (5–20 MPa for the walls at the UD, 15–25 MPa for the walls at the MD) occurs near 0·6–0·9D from the wall top. This occurrence can be explained by the shear force that gradually accumulates with the depth; thus, the vertical loads on the wall reach the maximum value at the neutral point, which further causes maximum vertical stress. The observed compressive stresses were basically within the acceptable range. The vertical stress distribution compared reasonably well to the previous studies (Dascal, 1979; Wen *et al.*, 2015; Yu *et al.*, 2015). The valley shape also affects the position of the maximum stress. For the V-shaped valley, most of the pressure in the wall is passed on to the bedrock, and eventually, the pressure delivered to the bottom decreases. The position of the maximum stress moves upward for the V-shaped valley. A large part of the dam body weight was transmitted by arching on both sides for the V-shaped valley, so the vertical stress also decreased.

In order to evaluate the behaviour of a cut-off wall for the concrete face rockfill dam, the authors have performed a three-dimensional finite-element analysis of the cut-off wall for Miaojiaba dam in Wen *et al.* (2015). The concrete cut-off wall was simulated using a linear elastic model. The behaviour of the soil–structure interface was modelled using a friction contact method, which regards the alluvium and the cut-off wall as two independent deformation bodies that follow the Coulomb friction law at the contact interface. Five rows of elements were divided in the thickness direction of the wall to reflect the behaviour more accurately. A total 6425 spatial eight-node isoparametric elements were utilised for the wall. The computational procedure followed the construction and subsequent reservoir filling process. Figure 12 shows the simulated minor principal stress distribution of the cut-off wall for Miaojiaba dam. For comparison, the minor principal stress distribution of a cut-off wall at the MD calculated by Yu *et al.* (2015) is presented in Figure 13.

For the Miaojiaba dam, at the EOC stage, the upstream face was in a compressive stress state, but tensile zones developed at the bottom and abutments in the downstream face. The major principal stress and minor principal stress were increased with the increase in the depth at maximum values of −20·0 and 1·9 MPa, respectively, which did not exceed the material strength. At the EOF stage, the bending downstream deformation reduced the tensile stress in the downstream face and it was converted nto a compressive stress state. The tensile stress also appeared at the bottom and abutments in the upstream face. The major and minor principal stresses reached the peak values of −22·0 and 2·0 MPa, respectively. These results showed that the wall undergoes significant tensile stress during both dam construction and reservoir filling, mainly caused by the restricted bending deformation and high elastic modulus of

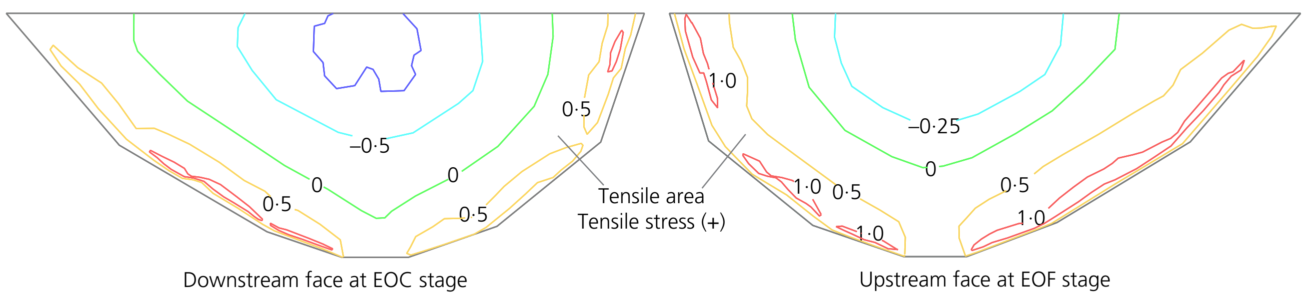

Figure 12. Simulated minor principal stresses distribution of the cut-off wall for Miaojiaba concrete face rockfill dam (unit: MPa)

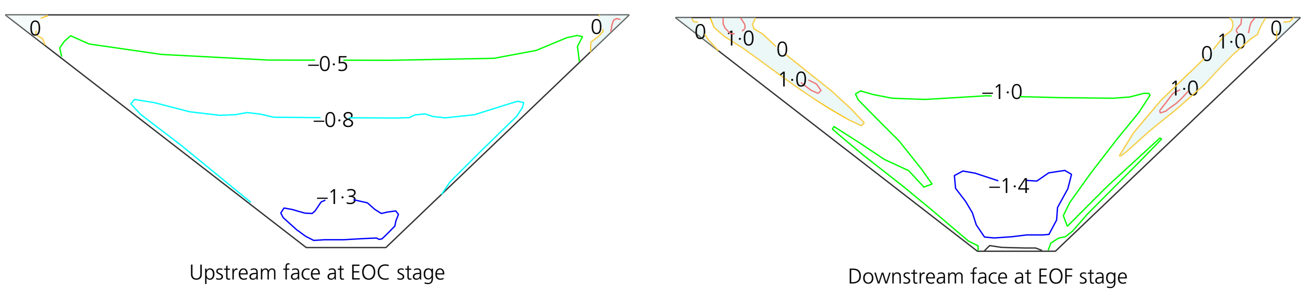

Figure 13. Simulated minor principal stresses distribution of a cut-off wall at the MD (unit: MPa) (modified from Yu *et al.* (2015))

Table 2. Maximum tensile and compressive vertical stress in several cut-off walls

Wall at the UD	At the EOC stage		At the EOF stage		Wall at the MD	At the EOC stage		At the EOF stage	
	Tensile: MPa	Compressive: MPa	Tensile: MPa	Compressive: MPa		Tensile: MPa	Compressive: MPa	Tensile: MPa	Compressive: MPa
Meixi	0·5	4·2	0·7	5·0	Xiabandi	—	7·9	—	10·1
Chahanwusu	0·2	6·7	0·6	10·0	Arminous	0·2	16·1	1·2	18·7
Hanpingzui	1·0	17·8	1·1	19·8	Taleghan	1·1	21·5	0·8	24·1
Miaojiaba	1·6	14·5	1·8	15·6	Pubugou	—	20·1	—	24·4

the wall. These stress distributions are significantly different from those for the wall at MD. As shown in Figure 13, the walls at the MD were mainly exposed to the compressive stress state, and tensile stress and the tensile region mainly appeared at the tip of the wall during dam construction; also the tensile area expanded at the abutments downstream owing to the bending effect at the EOF stage.

Table 2 shows the measured maximum vertical stress in several cut-off walls. It can be found that the walls at the UD mainly bear the bending effect under the load of water head and lateral earth pressure, and undergo significant tensile stress during both dam construction and reservoir filling. The walls at the MD, however, are principally subjected to a compression effect, which mainly exposes them to compressive stress states, and relatively smaller tensile stress was generated after reservoir filling. In addition, smaller stresses were observed in the walls constructed using PC (Xiabanda and Arminous).

6. Construction defects and cracking

The main problems of cut-off walls are defects during wall construction and cracking during dam construction and reservoir filling, causing leakage and deterioration of the seepage control system. Concrete wall construction defects have occurred in some existing dams (Rice and Duncan, 2010a). There are several forms of construction defects, including discontinuous construction joints, concrete segregations or soil inclusion, bottom sediment and concrete hollows (Ruffing *et al.*, 2015; Song and Cui, 2015). Construction defects are mainly caused by improper construction methods and material selection.

Cracking or failure of the concrete cut-off wall will occur when the compressive or tensile stresses induced in the wall exceed the capacity of the material. Rice and Duncan (2010b) reported that differential water pressure acting across the seepage barrier is of sufficient magnitude to cause cracking in the wall at MD, and the most likely location for the cracking is at the interface between the alluvium and the bedrock. Table 3 presents the failure or cracking of the cut-off wall for seven in-service dams. Failure observed in the wall for dams with core walls mainly presents as compressive failure. The failure was mainly observed at the bottom of the wall. For this wall type, the overlying earth pressure and shear force from the adjacent alluvium are the main causes of excessive compressive stress. Yu *et al.* (2015) analysed the tensile damage of the cut-off wall at MD and found that the tensile damage was mainly localised at the tip of the upper part of the wall. They concluded that the maximum tensile damage variable is small in the elements and no cracking will occur. For the walls of concrete face rockfill dams or dams with inclined walls, the failure mainly presents as tensile or shear cracks. The cracks occur at the top or bottom, where the wall comes into contact with bedrock. The bending deformation under the effect of water pressure induces tensile stresses on the wall, and the valley three-dimensional effect permits alluvium movements towards the centre of the

Table 3. Precedent concrete cut-off wall with failure or cracking

Project	Dam type and year	Depth and material	Issue	Cause
Arminous	DC, 1999	16 m, PC	Vertical joints cracks and erosion	Bentonite infill and internal erosion
Cetian	DC, 1989	39 m, OC	Cracks at the bottom after EOF	Deformation and compressive stress
Kezier	DI, 1998	40 m, OC	Some cracks at top after EOF	Bending deformation in downstream direction
Manic 3	DC, 1976	131 m, OC	Extrusion damage near bedrock after EOF	Inconsistent deformation of the wall and foundation
Niutoushan	CFRD, 1989	62·5 m, OC	Local damage and cracks at top	Bending deformation and tensile stress
Ravi	DI, 1968	88 m, OC	Shear and tensile damage at bottom after EOF	Longitudinal deflection deformation
Shawan	DC, 2000	64 m, OC	Infiltration damage at bottom during reservoir filling	Improper construction

CFRD, concrete face rockfill dam; DI, dams with inclined walls; DC, dams with core walls

wall, which could induce dragging of the wall at the abutments and thereby induce additional tensile stresses. These results are consistent with those of Brown and Bruggemann (2002), who reported that hydraulic fracture is more likely when a wall is used at UD due to the bending effect. In addition, cracking occurs mainly in OC walls and is rarely observed in PC walls.

7. Conclusions

This paper reports the statistical results relating to the behaviour of concrete cut-off wall from 43 case histories. The horizontal displacement, crest settlement, stress and cracking of the wall were studied. The effects of the wall location, wall material, foundation deformation characteristics and valley shape on behaviour were discussed. Based on the results, the following conclusions can be drawn.

(*a*) The cut-off wall generally bends upstream during dam construction and shifts towards the opposite direction during reservoir filling. The maximum displacement mainly occurs at the top and near the centre. The cut-off wall location is the deterministic factor affecting wall behaviour. The walls at MD generate a larger settlement during dam construction and then exhibit significant horizontal displacement after reservoir filling. However, the walls at UD generate a larger horizontal displacement, and the settlement is relatively small. The horizontal displacement for the wall at UD is between 0·07%D and 0·20%D at the EOC stage and between 0·05%D and 0·35%D at the EOF stage. The corresponding displacement for the wall at MD is 0·02% D to 0·07%D at the EOC stage and 0·05%D to 0·28%D at the EOF stage. Most of the settlement for the wall at MD is between 0·10%D and 0·24%D, which is significantly larger than the range of 0·02%D to 0·05%D for the wall at UD. The crest settlement is approximately 20% of the horizontal displacement for the wall at UD.

(*b*) The walls at MD are mainly exposed to compressive stress, which may induce compressive failure at the bottom. The walls at UD mainly bear the bending effect, and therefore undergo significant tensile stress. Tensile or shear cracks may occur at the bottom or at the abutments.

(*c*) The PC material can significantly improve the wall stress state. Wall deformation and stress in the V-shaped valley are smaller than in the U-shaped valley. The increase of the foundation deformation modulus could reduce the wall deformation and stress. The cut-off wall relative deformation decreases with the increase of the relative depth of the wall to the dam height.

Acknowledgements

This study was supported by the National Natural Science Foundation of China (51722907, 51679197, 51579207 and 51679193).

REFERENCES

Abbaslou H, Ghanizadeh AR and Amlashi AT (2016) The compatibility of bentonite/sepiolite plastic concrete cut-off wall material. *Construction and Building Materials* **124**: 1165–1173, https://doi.org/10.1016/j.conbuildmat.2016.08.116.

Arnold M, Beckhaus K and Wiedenmann U (2011) Cut-off wall construction using cutter soil mixing: a case study. *Geotechnik* **34(1)**: 11–21.

Ata AA, Salem TN and Elkhawas NM (2015) Properties of soil–bentonite–cement bypass mixture for cutoff walls. *Construction and Building Materials* **93**: 950–956, https://doi.org/10.1016/j.conbuildmat.2015.05.064.

Bagheri AR, Alibabaie M and Babaie M (2008) Reduction in the permeability of plastic concrete for cut-off walls through utilization of silica fume. *Construction and Building Materials* **22(6)**: 1247–1252.

Brown AJ and Bruggemann DA (2002) Arminous dam, Cyprus, and construction joints in diaphragm cut-off walls. *Géotechnique* **52(1)**: 3–13, http://dx.doi.org/10.1680/geot.2002.52.1.3.

Bruce DA, Dreese TL, Harris MC and Heenan DM (2012) Composite cut-off walls for existing dams: theory and practice. In *Proceedings of the 4th International Conference on Grouting and Deep Mixing, New Orleans, LA, USA* (Johnsen LF, Bruce DA and Byle MJ (eds)). American Society of Civil Engineers, Reston, VA, USA, GSP 228, vol. 2, pp. 1248–1264.

Brunner WG, Fiorotto R, Stötzer E and Schöpf M (2006) The innovative CSM-cutter soil mixing for constructing retaining and cut-off walls. In *Proceedings of the GeoCongress 2006: Geotechnical Engineering in the Information Technology Age, Atlanta, GA, USA* (DeGroot DJ, DeJong JT, Frost D and Baise LG (eds)). American Society of Civil Engineers, Reston, VA, USA, pp. 1–6.

CSHE (China Society for Hydropower Engineering) (2007) *Practice and Development of Building Dam with Overburden*. China

Hydropower Engineering Society of Hydraulic and Hydropower Station Buildings Professional Committee, China Water Conservancy and Hydropower Press, Beijing, China.
Dascal O (1979) Structural behaviour of the Manicouagan 3 cutoff. *Canadian Geotechnical Journal* **16(1)**: 200–221.
Dounias GT, Kountouris A and Anastasopoulos K (2012) Long-term behaviour of embankment dams: seven Greek dams. *Proceedings of the Institution of Civil Engineers – Geotechnical Engineering* **165(3)**: 157–177, http://dx.doi.org/10.1680/geng.11.00052.
Durgunoglu HT, Ikiz S, Eser S, Akcakal O and Sutman M (2012) A case study-installation of cut-off wall in Seyrantepe dam project. In *Proceedings of the 4th International Conference on Grouting and Deep Mixing, New Orleans, LA, USA* (Johnsen LF, Bruce DA and Byle MJ (eds)). American Society of Civil Engineers, Reston, VA, USA, GSP 228, vol. 2, pp. 1287–1293.
Fell R, Macgregor P, Stapledon D and Bell G (2005) *Geotechnical Engineering of Dams*. Balkema/Taylor & Francis, London, UK.
Gan L, Shen ZZ and Xu LQ (2014) Long-term deformation analysis of the Jiudianxia concrete-faced rockfill dam. *Arabian Journal for Science and Engineering* **39(3)**: 1589–1598.
Gao ZP (2000) *Dam Foundation Cut-Off Wall*. China Electric Power Press, Beijing, China.
Gikas V and Sakellariou M (2008) Settlement analysis of the Mornos earth dam (Greece): evidence from numerical modeling and geodetic monitoring. *Engineering Structures* **30(11)**: 3074–3081.
Gularte F, Barneich J, Burton J *et al.* (2007) First use of TRD construction technique for soil mix cutoff wall construction in the United States. In *Proceedings of Geo-Denver 2007: New Peaks in Geotechnics, Denver, CO, USA – Designing our Underground Space* (Ariaratnam ST (ed.)). American Society of Civil Engineers, Reston, VA, USA, GSP 174, pp. 1–12.
Hunter GJ (2003) *The Pre- and Post-Failure Deformation Behaviour of Soil Slopes*. University of New South Wales, Sydney, Australia.
Hinchberger S, Weck J and Newson T (2010) Mechanical and hydraulic characterization of plastic concrete for seepage cut-off walls. *Canadian Geotechnical Journal* **47(4)**: 461–471.
Hou YJ, Xu ZP and Liang JH (2004) Centrifuge modeling of cutoff wall for CFRD built in deep overburden. *Proceedings of International Conference on Hydropower, Yichang, China*. China Society for Hydropower Engineering, Beijing, China, pp. 86–92.
Kalkani EC and Michali AJ (1984) Steady flow calculations for cutoff wall depth variation. *Journal of Geotechnical Engineering* **110(7)**: 899–907.
King GJW and Collins P (1968) On the design of a rectangular dam with a central cut-off wall. *Géotechnique* **18(4)**: 489–498, http://dx.doi.org/10.1680/geot.1968.18.4.489.
Li NH, Mi ZK and Sun DW (2007) Study on affecting factors of stress-deformation of diaphragm walls for concrete face rockfill dams built on thick alluvium deposit. *Chinese Journal of Geotechnical Engineering* **29(1)**: 26–31.
Li YC, Cleall PJ, Wen YD, Chen YM and Pan Q (2015) Stresses in soil–bentonite slurry trench cut-off walls. *Géotechnique* **65(10)**: 843–850, http://dx.doi.org/10.1680/jgeot.14.P.219.
Moharrami A, Moradi G, Bonab MH, Katebi J and Moharrami G (2014) Performance of cutoff walls under hydraulic structures against uplift pressure and piping phenomenon. *Geotechnical and Geological Engineering* **33(1)**: 95–103.
O'Neal TS and Hagerty DJ (2011) Earth pressures in confined cohesionless backfill against tall rigid walls – a case history. *Canadian Geotechnical Journal* **48(8)**: 1188–1197.
Rice JD (2007) *A Study on the Long-Term Performance of Seepage Barriers in Dams*. Virginia Polytechnic Institute and State University, Blacksburg, VA, USA.
Rice JD and Duncan JM (2010a) Deformation and cracking of seepage barriers in dams due to changes in the pore pressure regime. *Journal of Geotechnical and Geoenvironmental Engineering* **136(1)**: 16–25.
Rice JD and Duncan JM (2010b) Findings of case histories on the long-term performance of seepage barriers in dams. *Journal of Geotechnical and Geoenvironmental Engineering* **136(1)**: 2–15.
Rosen JB, Arnold MA, Bachus RC and Schauer PED (2011) GIS for geotechnical decision making: visualization of cut-off wall construction data. In *Proceedings of Geo-Frontiers 2011 Congress: Advances in Geotechnical Engineering, Dallas, TX, USA* (Han J and Alzamora PE (eds)). American Society of Civil Engineers, Reston, VA, USA, GSP 211, pp. 2907–2916.
Ruffing DG, Evans JC and Ryan CR (2015) Strength and stress estimation in soil bentonite slurry trench cutoff walls using cone penetration test data. In *Proceedings of IFCEE, San Antonio, TX, USA* (Iskander M, Suleiman MT, Anderson JB and Laefer DF (eds)). American Society of Civil Engineers, Reston, VA, USA, GSP 256, pp. 2567–2576.
Singh AK, Mishra GC, Samadhiya NK and Ojha CSP (2006) Design of a rigid cutoff wall. *International Journal of Geomechanics* **6(4)**: 215–225.
Song H and Cui W (2015) Stop-end method for the panel connection of cut-off walls. *Proceedings of the Institution of Civil Engineers – Geotechnical Engineering* **168(5)**: 457–468, http://dx.doi.org/10.1680/jgeen.14.00086.
Soroush A and Soroush M (2005) Parameters affecting the thickness of bentonite cake in cutoff wall construction: case study and physical modeling. *Canadian Geotechnical Journal* **42(2)**: 646–654.
Wang QY, Sun WG and Xiong H (2008) *Plastic Concrete Cutoff Wall*. China Water Conservancy and Hydropower Press, Beijing, China.
WaterPower (1998) *Specification of Soil Test*, 1st edn. China WaterPower, Beijing, China, Specification SL-237.
Won MS and Kim YS (2008) A case study on the post-construction deformation of concrete face rockfill dams. *Canadian Geotechnical Journal* **45(6)**: 845–852.
Wen L, Qin Y, Chai J *et al.* (2015) Behaviour of concrete-face rockfill dam on sand and gravel foundation. *Proceedings of the Institution of Civil Engineers – Geotechnical Engineering* **168(5)**: 439–456, http://dx.doi.org/10.1680/jgeen.14.00103.
Wen L, Chai J, Xu Z, Qin Y and Li Y (2017) Monitoring and numerical analysis of behaviour of Miaojiaba concrete-face rockfill dam built on river gravel foundation in China. *Computers and Geotechnics* **85**: 230–248, https://doi.org/10.1016/j.compgeo.2016.12.018.
Xiao M, Ledezma M and Wang J (2016) Reduced-scale shake table testing of seismic behaviors of slurry cutoff walls. *Journal of Performance of Constructed Facilities* **30(3)**: 04015057.
Yu X, Kong X, Zou D, Zhou Y and Hu Z (2015) Linear elastic and plastic-damage analyses of a concrete cut-off wall constructed in deep overburden. *Computers and Geotechnics* **69**: 462–473, https://doi.org/10.1016/j.compgeo.2015.05.015.

How can you contribute?

To discuss this paper, please email up to 500 words to the editor at journals@ice.org.uk. Your contribution will be forwarded to the author(s) for a reply and, if considered appropriate by the editorial board, it will be published as discussion in a future issue of the journal.

Proceedings journals rely entirely on contributions from the civil engineering profession (and allied disciplines). Information about how to submit your paper online is available at www.icevirtuallibrary.com/page/authors, where you will also find detailed author guidelines.